

# Preparation and properties of the main-chain-fluorinated thermoplastic polyurethane elastomer

Pengfei Liu · Lin Ye · Yonggang Liu · Fude Nie

Received: 30 March 2010 / Revised: 1 July 2010 / Accepted: 8 July 2010 /  
Published online: 16 July 2010  
© Springer-Verlag 2010

**Abstract** A series of main-chain-fluorinated thermoplastic polyurethane elastomers (FTPU) based on fluoropoly(oxyalkylene)diol (FPOA) were prepared by a one-step bulk polymerization. Polybutylene adipate (PBA) was combined with FPOA as a soft-segment in order to improve the solvent solubility of FTPU. The effects of the mass ratio of FPOA/PBA and the mass fraction of hard-segment on the mechanical properties of FTPU were investigated. The structure and morphology of FTPU were characterized by FTIR, GPC, DMA, surface property, and AFM analysis. The results indicated that the tensile strength and elongation at break for the sample of FTPU with FPOA/PBA ratio 30/70 can reach as high as 36.6 MPa and 1228.1%, respectively. It exhibited relatively high molecular weight, high damping property, enhanced thermal stability, and extremely low surface tension. The introduction of fluorinated blocks made the extent of incompatibility of the two phases of FTPU greater and the trend of micro-phase separation more serious.

**Keywords** Fluorinated thermoplastic polyurethane elastomers (FTPU) · Mechanical properties · Thermal stability · Surface tension · Phase separation

## Introduction

By introducing fluorinated blocks into the molecular chains of thermoplastic polyurethane elastomer (TPU), the resulting fluorinated thermoplastic polyurethane elastomers (FTPU) not only maintain most of the outstanding properties of TPU,

---

P. Liu · L. Ye (✉)

State Key Laboratory of Polymer Materials Engineering, Polymer Research Institute of Sichuan University, Chengdu 610065, China  
e-mail: yelinwh@126.com

Y. Liu · F. Nie

China Academy of Engineering Physics, Mianyang 621014, China

such as high strength, high toughness, and high damping properties, but also offer the basic advantages of improved solvent and chemical resistance, a lower surface tension, and low coefficient of friction, resulting in wide applications in the areas of coatings, leather decoration, textiles, and medicine [1–5].

There are, however, only a few examples of commercially available fluorinated elastomers, such as the crosslinkable copolymers of vinylidene fluoride or tetrafluoroethylene with a few suitable fluorinated comonomers like hexafluoropropene or perfluorovinylethers. For example, in the fluorinated thermoplastic elastomer recently developed by Daikin, the soft phase is the vinylidene fluoride-hexafluoropropene copolymer [6, 7]. The use of short fluorinated chain extenders does not offer any advantage in terms of the surface properties and elastomeric properties. No additional research was found for other kinds of fluorinated thermoplastic elastomers. The main reason is, perhaps, the very limited availability of suitable fluorinated monomers or macromers [8].

At present, FTPU are mainly applied as bio-medicine materials. However, the low reaction activity of the fluorinated monomers led to low molecular weight and poor mechanical properties of the resulting products, which restricted the wide applications of FTPU. The  $\overline{M}_n$  of the reported FTPU were about  $2\text{--}3 \times 10^4$ , and the tensile strength and elongation at break can reach nearly 10–20 MPa and 300–500%, respectively [9]. However, Ausimont (Bussi, Italy) has produced the poly(fluoroxyalkylene)diol with relatively high molecular weight, and the functional end groups allow them to be a candidate as a conventional polyester or polyether as the soft-segment of the traditional TPU. The aim of this work was to synthesize FTPU with such fluoropolydiol, so that the main-chain of the polymer contained high amount of fluorinated blocks, with the hope some unique properties such as improved mechanical properties, low surface tension and high temperature performance could be achieved. Moreover, the completely linear FTPU with excellent solubility was prepared for the purpose of potential adhesives and coating applications.

## Experimental

### Materials

The fluoropoly(oxyalkylene)diol (FPOA) from Ausimont (Bussi, Italy) used in the present work consisted of a random distribution of  $-\text{CF}_2\text{CF}_2\text{O}-$  and  $-\text{CF}_2\text{O}-$  groups, end capped by ethoxylated units  $-\text{CH}_2\text{OH}$ ,  $\overline{M}_n = 700$ . Diphenylmethane diisocyanate (MDI) from Wanhua Polyurethane Co. Ltd (Yantai, China) was used as received; 1,4-butanediol (BDO) was supplied by Bodi Chemical Co. Ltd. (Tianjin, China); polybutylene adipate glycol (PBA) ( $\overline{M}_n$ , 2000) was purchased from Huada Chemical Engineering Co. Ltd (Yantai, China).

### Synthesis of fluorinated thermoplastic polyurethane elastomer (FTPU)

A one-step procedure was adopted to prepare FTPU via bulk polymerization. The stoichiometric amounts of the FPOA and PBA were mixed and dried under vacuum

at 100 °C for 2 h. Then an appropriate amount of BDO was added into this bulk by vigorously stirring. At a chosen temperature, the calculated amount of reactant (MDI) was added to give a final NCO/OH ratio of 0.98, resulting in a polymer with a linear chain. Finally the product was cast in a mold at a chosen temperature for 1 h. The samples were conditioned for 1 week at room temperature before testing. The hard-segment of this product was composed of diisocyanate and the chain extender, and the soft-segments originated from the polyols.

## Measurements

### *FTIR analysis*

The compositions of the synthesized FTPU were analyzed with a Nicolet-560 Fourier-transform infrared spectrometer (FTIR) (USA). The specimen was prepared by casting a polymer film from solution on KBr discs. The scanning rate was 20 min<sup>-1</sup>.

### *GPC analysis*

The number ( $\overline{Mn}$ ) and weight ( $\overline{Mw}$ ) average molecular weights, and the index of the molecular weight distribution ( $\overline{Mw}/\overline{Mn}$ ) of FTPU were measured by gel permeation chromatography (GPC) with a Waters 150-C instrument (USA) at 30 °C. Tetrahydrofuran (THF) was used as an eluent (flow rate = 1 mL/min).

### *Tensile properties*

The tensile properties of the samples were measured with a 4,302 material testing machine from Instron Co. (USA) according to ISO527/1-1993 (E). The tensile speed and temperature were 200 mm/min and 23 °C, respectively.

### *DMA analysis*

The dynamic mechanical analysis (DMA) was carried out using a TA Instrument Q800 DMA (USA). All the samples were measured with a single cantilever mode at a heating rate of 10 °C/min and a frequency of 30 Hz. The sample size was 35 × 1 × 0.2 mm<sup>3</sup>.

### *TGA analysis*

The thermo-gravimetric analysis (TGA) was performed with a TA2950 thermobalance from TA Co. (U.S.A.) under nitrogen atmosphere with the flow rate of 50 mL/min. The granulated samples of about 10 mg were heated from ambient temperature to approximately 650 °C at a heating rate of 10 °C/min. All samples were dried in the heating oven at 80 °C for 2 h before the measurement.

### Contact angle

The contact angles of water and glycerol as testing liquids on FTPU were measured by an ErmaG-1 contact angle test apparatus (Japan) at room temperature using the sessile drop method.

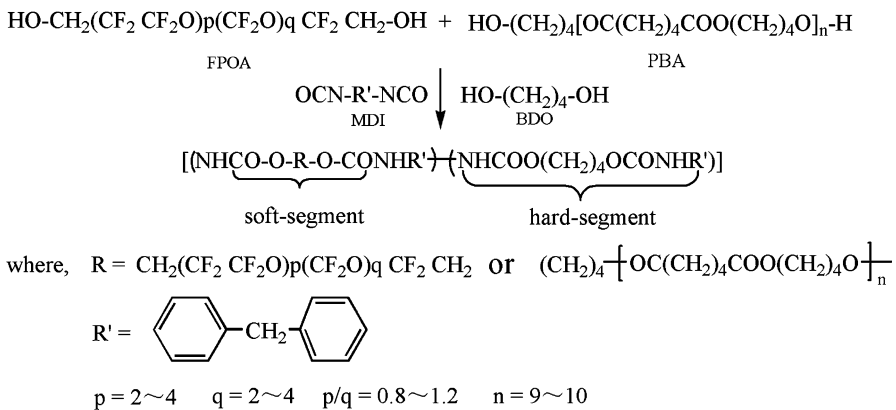
### AFM analysis

The images of FTPU were visualized on a Digital Instruments Nanoscope IIIa AFM microscopy (USA) by tapping-mode. The sample was dissolved in THF and coated on a mica substrate, and then dried in vacuum at 60 °C for 12 h. It was measured in air at room temperature with a scanning area of 50 μm.

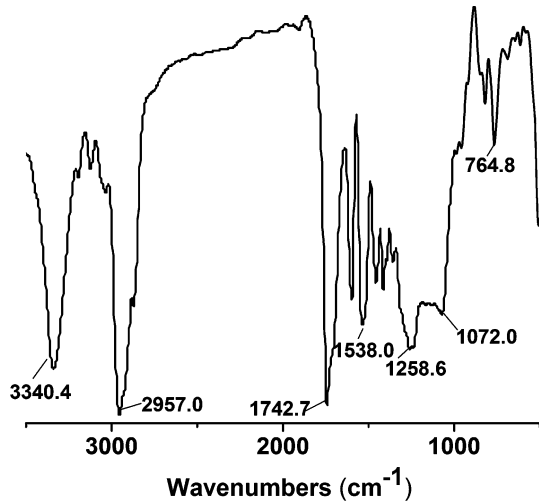
### Results and discussion

The reaction equations for FTPU synthesized in this study are shown in Scheme 1.

The composition of FTPU was analyzed by FTIR. As shown in Fig. 1, there was a strong N–H stretching vibration absorption peak at 3340.4 cm<sup>-1</sup>, and –CH<sub>2</sub>– stretching vibration absorption peak at 2957.0 cm<sup>-1</sup>; a C=O stretching peak was observed at 1742.7 cm<sup>-1</sup>; the peak at 1538.0 cm<sup>-1</sup> was assigned to N–H bending vibration absorption or the stretching vibration of the phenyl framework; the stretching vibration peak of C–O–C was in the range of 1,100–1258.6 cm<sup>-1</sup>; and the absorption peak at 1072.0 cm<sup>-1</sup> was attributed to the stretching vibration of C–F. The absorption peak of diisocyanate (–N=C=O) band at 2,250–2,275 cm<sup>-1</sup> was absent in the spectra of the FTPU, indicating that this group was completely consumed in the reaction [10].



**Scheme 1** Reaction equation of FTPU

**Fig. 1** FTIR spectrum of FTPU

### Relationship between the chemical structure and mechanical property of FTPU

The mechanical properties of FTPU are related with its chemical bonds, intermolecular forces, and molecular weight. It is primarily determined by the chemical structure of the soft-segments and hard-segments.

Although FTPU possesses a completely linear chain structure, the form with only FPOA and no PBA can only dissolve in a few solvents, and presents poor solvent solubility. In order to improve the solvent solubility of FTPU, PBA was combined with FPOA as the soft-segments of FTPU. In the range of the mass ratio of FPOA/PBA from 10/90 to 30/70, the FTPU can dissolve in tetrahydrofuran, *N,N*-Dimethyl formamide, etc. Above the mass ratio of 30/70 of FPOA/PBA, the product of FTPU can only swell in these solvents.

As shown in Fig. 2, the GPC curves of FTPU synthesized with 30 wt% of mass fraction of hard-segment and varying mass ratio of FPOA/PBA were single bell-shapes without a distribution peak for small-molecular substances, indicating that FPOA and PBA were all consumed to obtain the final product. The related results are listed in Table 1. The samples of FTPU had relatively high molecular weight. With the increase of the fluorine content, the elution time of FTPU increased and there was small drop of the molecular weight without much influence on the molecular weight distribution.

The fluorine content had a large influence on the mechanical properties of FTPU. As shown in Fig. 3, for FTPU with 30 wt% hard-segment, with the increase of the mass ratio of FPOA/PBA, the mechanical strength and toughness of FTPU increased. Stress-whitening during tensile test can also be observed. The tensile strength and elongation at break for the sample of FTPU with FPOA/PBA ratio 30/70 reached as high as 36.6 MPa and 1228.1%, respectively. The high symmetry and flexibility of the molecular chain of fluorinated polydiol facilitated to crystallize of the soft-segment and contributed to the high tensile strength and toughness of FTPU.

**Fig. 2** GPC curves of FTPU with varying mass ratio of FPOA/PBA. 1 FPOA/PBA (10/90); 2 FPOA/PBA (20/80); 3 FPOA/PBA (30/70)

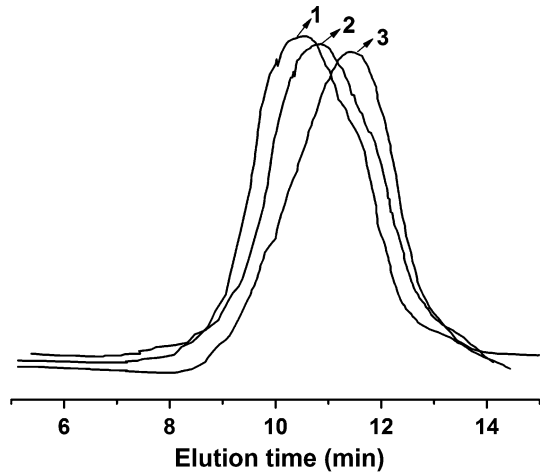


**Table 1** GPC result of FTPU with varying mass ratio of FPOA/PBA (Mass fraction of hard-segment: 30 wt%)

FTPU	Mass ratio of FPOA/PBA	Fluorine content (%)	Retention time (min)	$\overline{M}_n (\times 10^4)$	$\overline{M}_w (\times 10^4)$	$\overline{M}_w/\overline{M}_n$
1	10/90	7	10.54	6.32	18.38	2.9
2	20/80	14	10.64	5.07	15.94	3.1
3	30/70	21	11.44	5.11	13.13	2.6

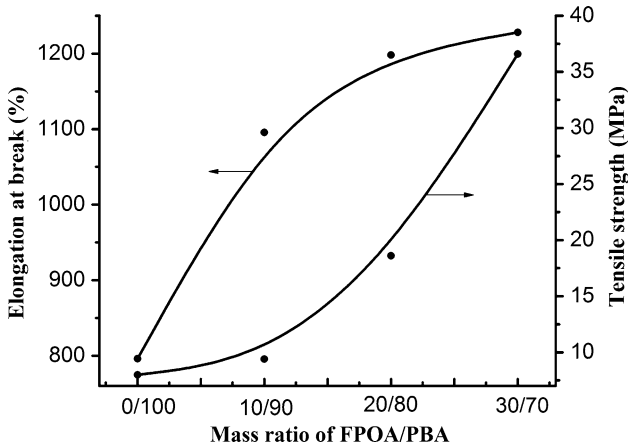


**Fig. 3** Mechanical property of FTPU with varying mass ratio of FPOA/PBA

As shown in Fig. 4, for FTPU with FPOA/PBA mass ratio 20/80, the tensile strength increased with the mass fraction of hard-segment, and a slight increase of the elongation at break was observed. The sample with high mass fraction of

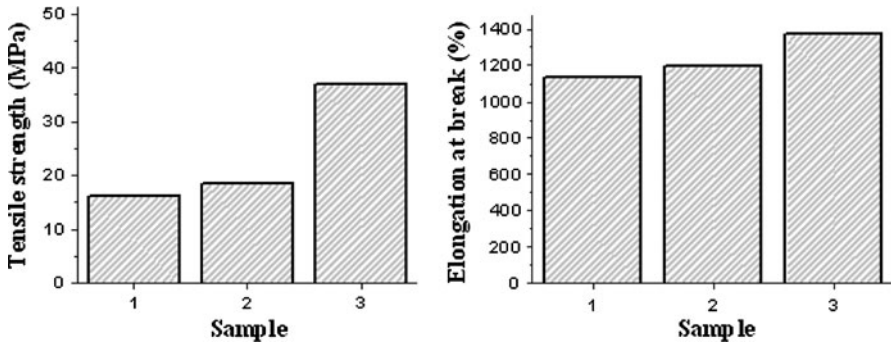


**Fig. 4** Mechanical properties of FTPU with varying content of hard-segment. 1 20 wt% of hard-segment; 2 30 wt% of hard-segment; 3 40 wt% of hard-segment

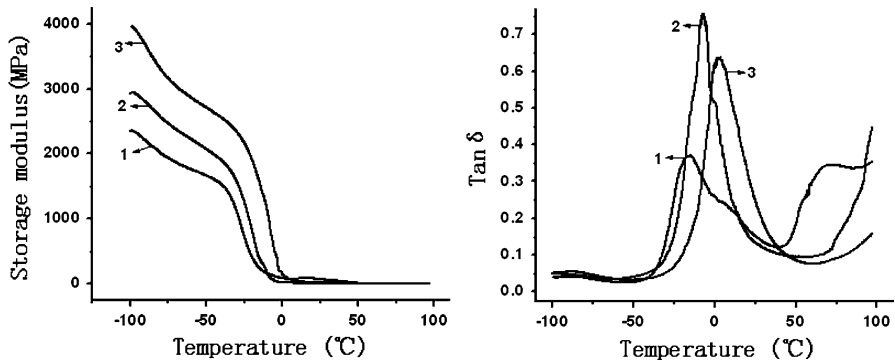


**Fig. 5** Damping properties of FTPU with varying mass fraction of hard-segment. 1 20 wt% of hard-segment; 2 30 wt% of hard-segment; 3 40 wt% of hard-segment

hard-segment possessed more physical crosslinking points and rigid groups, resulting in the enhancement of rigidity of the macromolecular chain of FTPU.

#### Dynamic mechanical property of FTPU

Dynamical mechanical analysis provides information on the glass transition and damping properties of a polymer. The dynamical mechanical properties of FTPU with FPOA/PBA mass ratio 20/80 and varying mass fraction of hard-segment are shown in Fig. 5. The storage modulus increased with the mass fraction of hard-segment. All the samples exhibited two loss peaks corresponding to the glass transition temperatures of the soft-segment composed of FPOA ( $T_{gb}$ ), and PBA ( $T_{ga}$ ), respectively, indicating that the PBA soft chains were mutually incompatible with the FPOA soft chains, and a multiphase structure was formed. This segregation was promoted by the strong difference in the solubility parameters between the PBA soft chain and the FPOA soft chain, which could be calculated to be 9.57 and 6.82  $(\text{cal}/\text{cm}^3)^{1/2}$ , respectively. The loss peaks corresponding to the PBA block ( $T_{ga}$ ) shifted to higher temperature with the increase of the mass fraction of hard-segment,

while the glass transition temperature of the soft-segment of FPOA block ( $T_{gb}$ ) had a slight decrease. The result can be considered due to the constraint given by chemical links with the hard phase, which reduced the degree of freedom of the soft chains. Numerical DMA data of FTPU were listed in Table 2. Generally, the damping properties of TPU decreased with the mass fraction of hard-segment, because it was the soft-segment that endowed it with the damping property. However, for FTPU, the introduction of the fluorinated polydiol blocks, perhaps, resulted in the increase of the value of  $\tan\delta$  with the mass fraction of hard-segment.

The dynamical mechanical properties of FTPU with 30 wt% hard-segment and varying mass ratio of FPOA/PBA are shown in Fig. 6, and the relevant data are collected in Table 3. The storage modulus increased with the fluorinated polydiol content. With the increase of fluorinated polydiol content, the loss peak corresponding to the glass transition temperature of the FPOA block ( $T_{gb}$ ) soft-segment shifted to lower temperature, and the loss peak corresponding to the PBA block ( $T_{ga}$ ) shifted to higher temperature, indicating the increased phase segregation. All samples of FTPU had a high damping factor ( $\tan\delta$ ), which decreased with the fluorine content [11].

### Thermal stability of FTPU

TGA is an important method for the study on the thermal stability of a polymer. The TGA curves of TPU with the soft-segment completely composed of PBA, and

**Table 2** DMA parameters of FTPU with varying mass fraction of hard-segment

FTPU	Mass ratio of FPOA/PBA	Mass fraction of hard-segment (%)	Soft-segment		$\tan\delta_{\max}$	$T_{\tan\delta > 0.3}$ (°C)
			$T_{gb}$ (°C)	$T_{ga}$ (°C)		
1	20/80	20	-81.42	-15.25	0.37	-23.39 to -6.44
2		30	-83.24	-10.09	0.76	-20.48 to 7.36
3		40	-85.26	2.97	0.63	-7.80 to 21.30

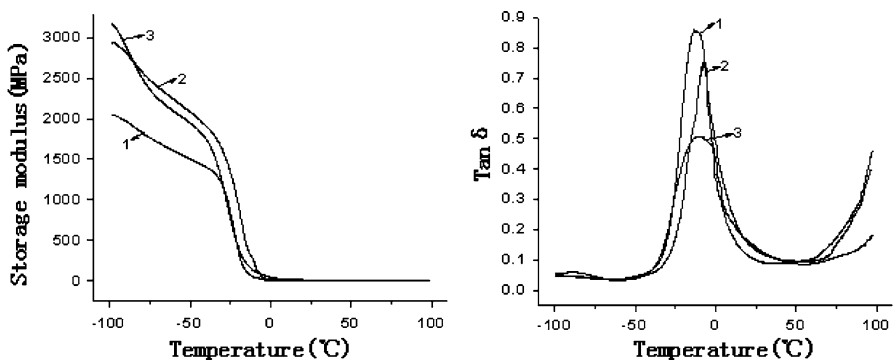


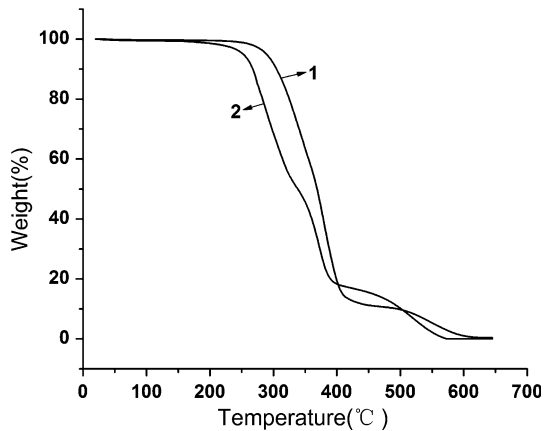
**Fig. 6** Damping properties of FTPU with varying mass ratio of FPOA/PBA. 1 FPOA/PBA (10/90); 2 FPOA/PBA (20/80); 3 FPOA/PBA (30/70)



**Table 3** DMA parameters of FTPU with varying mass ratio of FPOA/PBA

FTPU	Mass ratio of FPOA/PBA	Fluorine content (%)	Soft-segment		Tanδ <sub>max</sub>	T <sub>Tanδ &gt; 0.3</sub> (°C)
			T <sub>gb</sub> (°C)	T <sub>ga</sub> (°C)		
1	10/90	7	-81.96	-10.95	0.85	-24.11 to 6.56
2	20/80	14	-83.24	-10.09	0.76	-20.48 to 7.36
3	30/70	21	-85.63	-9.68	0.51	-23.85 to 5.70

**Fig. 7** Thermogravimetric analysis of FTPU and TPU. 1 FTPU, 30 wt% of hard-segment, FPOA/PBA = 30/70; 2 TPU, 30 wt% of hard-segment, FPOA/PBA = 0/100



FTPU with the soft-segment composed of FPOA/PBA (30/70) are shown in Fig. 7. The mass fraction of hard-segment for both was 30 wt%. The thermal degradation characteristic temperatures such as  $T_{onset}$  and  $T_{end}$  represent the temperature at the intersection point of the tangent line at the fastest thermal weight loss rate with the extension line for the start and end of the degradation.  $V_{max}$  and  $T_{peak}$  are, respectively, the maximal thermal degradation rate and the temperature at this point.  $T_{5\%}$ ,  $T_{20\%}$ , and  $T_{50\%}$  are the temperatures of the samples with the weight loss of 5, 20, and 50%, respectively.

As listed in Table 4, the thermal degradation characteristic temperatures of FTPU was higher by over 30 °C than that of the sample of TPU, indicating that FTPU, by introduction of fluorinated blocks into the backbone, exhibited remarkable thermal stability.

### Surface property of FTPU

The surface tension of a solid ( $\gamma_s$ ) contains both a polarity component ( $\gamma_s^p$ ) and a dispersion component ( $\gamma_s^d$ ) [12, 13].

$$\gamma_s = \gamma_s^p + \gamma_s^d \tag{1}$$

$\gamma_s^p$  and  $\gamma_s^d$  can be calculated from the geometric-mean equation [14]:

$$\gamma_{LV}(1 + \cos\theta) = 2(\gamma_L^d \gamma_s^d)^{1/2} + 2(\gamma_L^p \gamma_s^p)^{1/2} \tag{2}$$

**Table 4** TGA characteristic parameters of FTPU and TPU

Sample	$T_{\text{onset}}$ (°C)	$T_{\text{peak}}$ (°C)	$T_{\text{end}}$ (°C)	$T_{5\%}$ (°C)	$T_{20\%}$ (°C)	$T_{50\%}$ (°C)	$V_{\text{max}}$ (%/°C)
FTPU	324	521	403	289	325	369	0.17
TPU	257	380	387	252	283	338	1.09

**Table 5** Surface tension of test liquids (20 °C)

Testing liquid	$\gamma_{\text{LV}}$ (mN/m)	$\gamma_{\text{L}}^{\text{d}}$ (mN/m)	$\gamma_{\text{L}}^{\text{p}}$ (mN/m)
Water	72.8	21.8	51.0
Glycerol	63.4	37.0	26.4

**Table 6** Contact angle of testing liquids on FTPU and the surface tension

FTPU	Mass fraction of FPOA/PBA	Fluorine content (%)	Contact angle (°)		$\gamma_{\text{s}}^{\text{d}}$ (mN/m)	$\gamma_{\text{s}}^{\text{p}}$ (mN/m)	$\gamma$ (mN/m)
			Water	Glycerin			
1	0/100	0	52.7	61.9	2.8	50.4	53.2
2	10/90	7	91.7	97.4	0.6	19.7	20.3
3	20/80	14	93.5	99.3	0.5	18.7	19.2
4	30/70	21	95.2	101.1	0.4	17.7	18.1

In the equation,  $\theta$  is contact angle;  $\gamma_{\text{LV}}$  is surface tension of test liquid;  $\gamma_{\text{L}}^{\text{p}}$  and  $\gamma_{\text{L}}^{\text{d}}$  are polarity component and dispersion components of the test liquid, respectively;  $\gamma_{\text{s}}^{\text{p}}$  and  $\gamma_{\text{s}}^{\text{d}}$  are polarity component and dispersion component of the solid, respectively.

Water and glycerin were selected as the test liquids; their surface tensions are listed in Table 5. The surface tensions of FTPU with 30 wt% hard-segment and varying mass fractions of FPOA/PBA were calculated with the geometric-mean equation. As listed in Table 6, with the increase of fluorine content, the contact angle of water and glycerin on the surface of the sample of FTPU increased, and the surface tension of FTPU decreased from 53.2 to 18.1 mN/m.

### Aggregation morphology of FTPU

The molecular chains of FTPU are composed of two soft-segments originating from the two polyols, and the hard-segment originating from diisocyanate and the chain extender. Ideally, the two segments are immiscible and phase separation occurred during the formation of morphology.

The multi-phase nature of FTPU has been strongly implied from AFM analysis [15, 16]. Figure 8 shows the height image, phase image and 3D image of FTPU with 30 wt% hard-segment and 30/70 FPOA/PBA mass ratio. The scope of observation was 50  $\mu\text{m}$ . A typical two phase structure can be observed. The comparatively bright part corresponds to the microphase of the aggregated hard-segments of FTPU, and the grey part corresponds to the microphase of the two aggregated

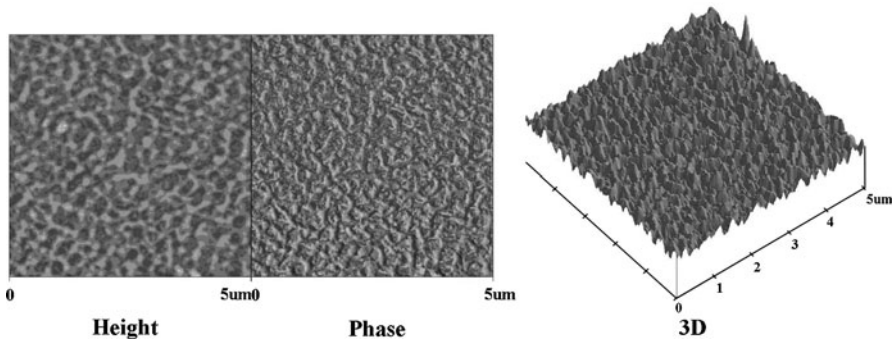


**Fig. 8** AFM images of micro-phase separation of FTPU with 30 wt% of hard-segment and 30/70 FPOA/PBA mass ratio (The observation domain: 5  $\mu\text{m}$ )

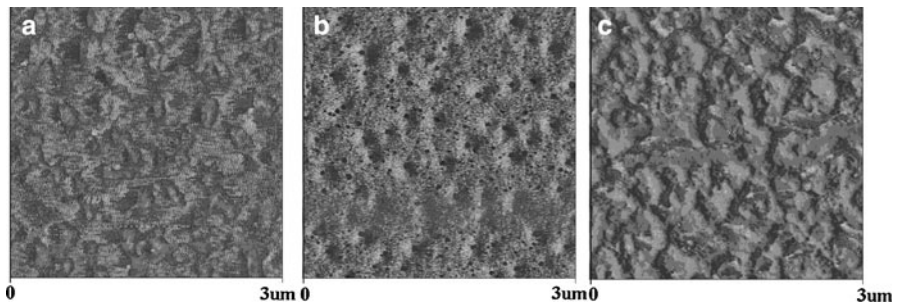


**Fig. 9** AFM phase images of FTPU with 30 wt% of hard-segment and varying mass ratio of FPOA/PBA. **a** FPOA/PBA (10/90); **b** FPOA/PBA (20/80); **c** FPOA/PBA (30/70)

soft-segments of FTPU. In the 3D image, it can be seen that a lot of bright bumps were embedded in the grey substrate. Lots of “wave troughs” corresponding to the soft-segments and lots of “wave crests” corresponding to the hard-segment indicated that there was a remarkable micro-phase separation in the molecules of FTPU. The soft-segment formed the continuous phase and the hard-segment formed the dispersion phase. Although the soft-segments of FTPU were composed of FPOA and PBA block phase, as indicated by DMA result, FPOA phase was too small to be observed due to its low molecular weight and low content. Therefore, the soft-segment of FTPU can only present one phase state. However, with increasing FPOA/PBA mass ratio, the introduction of fluorinated blocks made the extent of incompatibility of the two phases greater and the trend of micro-phase separation more serious, as shown in Fig. 9.

## Conclusions

A one-step procedure was adopted to synthesize FTPU via bulk polymerization. PBA was combined with FPOA as the soft-segments of FTPU in order to improve

the solvent solubility of FTPU. The samples of FTPU had relatively high molecular weight. With the increase of the mass ratio of FPOA/PBA, the mechanical strength and toughness of FTPU increased. The tensile strength and elongation at break for the sample of FTPU with FPOA/PBA ratio 30/70 can reach as high as 36.6 MPa and 1228.1%, respectively, compared to the reported FTPU with only 10–20 MPa of tensile strength and 300–500% of elongation at break [9]. The storage modulus increased with the mass ratio of FPOA/PBA and mass fraction of hard-segment. All the samples exhibited two loss peaks corresponding to the glass transition temperatures of the soft-segments composed of FPOA ( $T_{gb}$ ), and PBA ( $T_{ga}$ ), respectively, which shifted to higher temperature with the decrease of the mass ratio of FPOA/PBA and increase of the mass fraction of hard-segment. The samples of FTPU had a high damping factor ( $\tan\delta$ ). The thermal degradation characteristic temperatures of FTPU with FPOA/PBA ratio 30/70 were higher by over 30 °C than that of the sample of TPU with the soft-segment completely composed of PBA, indicating that FTPU, by introduction of fluorinated blocks into the backbone, exhibited improved thermal stability. With the increase of fluorine content, the surface tension of FTPU decreased from 53.2 to 18.1 mN/m. The introduction of fluorinated blocks made the extent of incompatibility of the two phases greater and the trend of micro-phase separation more serious.

**Acknowledgment** This study was supported by Natural Science Fund of China (10676024).

## References

1. Li S, Liu Y (2002) Polyurethane resin and application. Chemical Engineering Publisher, Beijing
2. Frick A, Rochman A (2004) Characterization of TPU-elastomers by thermal analysis (DSC). *Polym Test* 23(4):413–417
3. Rogulska M, Podkoscielny W, Kultys A, Pikus S, Pozdzik E (2006) Studies on thermoplastic polyurethanes based on new diphenylethane-derivative diols. 1. Synthesis and characterization of nonsegmented polyurethanes from HDI and MDI. *Eur Polym J* 42(8):1786–1797
4. Yeganeh H, Barikani M, Khodabadi FN (2000) Synthesis and properties of novel thermoplastic poly(urethane-imide)s. *Eur Polym J* 36(10):2207–2211
5. Cao Q, Li Y, Jing B, Liu PS (2006) Structure and mechanical properties of thermoplastic polyurethane, based an hyperbranched polyesters. *J Appl Polym Sci* 102(6):5266–5273
6. Tonelli C, Ajroldi G (2003) New fluoro-modified thermoplastic polyurethanes. *J Appl Polym Sci* 87(14):2279–2294
7. Hung MH, Farnham WB, Feiring AE, Rozen S (1993) A new synthetic approach to poly- and perfluorinated polyethers. *J Am Chem Soc* 115(20):8954–8959
8. Yoon SC, Sung YK, Ratner BD (1990) Surface and bulk structure of segmented poly(ether urethanes) with perfluoro chain extenders. 4. Role of hydrogen bonding on thermal transitions. *Macromolecules* 23(20):4351–4356
9. Tonelli C, Trombetta T, Scicchitano M, Simeone G, Ajroldi G (1996) New fluorinated thermoplastic elastomers. *J Appl Polym Sci* 59(2):311–327
10. Guelcher SA, Gallagher KM, Didier JE, Klinedinst DB, Doctor JS, Goldstein AS, Wilkes GL, Beckman EJ, Hollinger JO (2005) Synthesis of biocompatible segmented polyurethanes from aliphatic diisocyanates and diurea diol chain extenders. *Acta Biomater* 1(4):471–484
11. Oertel G (1989) Polyurethane handbook. Hanser Publishers, Munich
12. Kwok DY, Neumann AW (2000) Characterization of the surface free energy of cellulose ether films. *Colloids Surf A* 161(1):31–48

13. Sharma PK, Hanumantha RK (2002) Analysis of different approaches for evaluation of surface energy of microbial cells by contact angle goniometry. *Adv Colloids Interface Sci* 98(1):341–463
14. Sikka M, Singh N, Karim A, Bates FS (1993) Entropy-driven surface segregation in block copolymer melts. *Physical Review Letters* 3(70):307–310
15. Mclean S, Scott S, Bryan B (1997) Tapping-mode AFM studies using phase detection for resolution of nanophases in segmented polyurethane and other block copolymer. *Macromolecules* 30(26): 8314–8317
16. Reifer D, Windeit R, Kumpf RJ (1995) AFM and TEM investigations of polypropylene/polyurethane blends. *Thin Solid Films* 264(2):148–152